PROCEEDINGS OF SCIENCE

The polarized hydrogen jet target measurements at RHIC

A. Poblaguev*†, E. Aschenauer, G. Atoian, A. Basilevsky A. Dion, K. O. Eyser, H. Huang, Y. Makdisi, W. Schmidke, D. Smirnov, K. Yip, A. Zelenski
Brookhaven National Laboratory, Upton, NY, 11973

I. Alekseev, D. Svirida

Institute for Theoretical and Experimental Physics,Moscow, 117218, Russia

D. Kalinkin

Moscow Institute of Physics and Technology, Dolgoprudny, Moscow region, 141700, Russia

The polarized atomic hydrogen gas jet target polarimeter (H-Jet) at the Relativistic Heavy Ion Collider (RHIC) polarized proton complex [1] is employed for the absolute polarization measurement in both RHIC beams. The beam polarization is determined by measuring the asymmetry of low energy (1–5 MeV) recoil proton production in the Coulomb Nuclear Interference (CNI) region. With analyzing power of such a process of about 4%, the average beam polarization is measured with statistical accuracy of about $\delta P \sim 3\%$ during an 8-hour store in RHIC. Calibration of the H-Jet Si detectors and systematic errors of the measurements are discussed.

XVth International Workshop on Polarized Sources, Targets, and Polarimetry,
September 9-13, 2013
Charlottesville, Virginia, USA

*Speaker.
†E-mail: `poblaguev@bnl.gov`

PoS(PSTP 2013)055

1. Introduction

Proton beam polarization measurement is an important element of the RHIC [1] polarized proton program. The H-Jet polarimeter [2] is employed to measure the average polarization of both RHIC beams, *Blue* and *Yellow*. Schematically, the H-Jet polarimeter consists of a jet-target atomic beam and six 16-channel silicon detectors as shown on Fig. 1.

At the H-Jet location, the Blue and Yellow RHIC beams are vertically separated, so the polarization of both beams can be measured simultaneously. In each detector, 8 strips are designated to detect recoil protons produced by Blue beam and eight strips to detect Yellow beam recoil protons.

Determination of the beam polarization is based on the measurement of the asymmetry of low energy (CNI region) recoil proton production in elastic $p^{\uparrow}p^{\uparrow}$ scattering. Since both, the proton beam and the jet target, polarizations are flipping, we can measure concurrently the asymmetry relative to the beam and jet polarity:

$$a_{\text{beam}} = A_N P_{\text{beam}}, \qquad a_{\text{jet}} = A_N P_{\text{jet}} \tag{1.1}$$

Since the event selection is identical for the both studies, the average value of analyzing power A_N is the same for the beam and jet asymmetry measurements. As a result, beam polarization may be related to the jet one

$$P_{\text{beam}} = \frac{a_{\text{beam}}}{a_{\text{jet}}} P_{\text{jet}}. \tag{1.2}$$

The average proton polarization in the jet $P_{\text{jet}} \approx 92\%$ is derived from the hydrogen atomic gas polarization measurements by a Breit-Rabi polarimeter. For the recoil proton energy range of 1–5 MeV, the average value of analyzing power is about $A_N \sim 0.04$ as shown in Fig 2 . In the recent RHIC runs, the proton beams polarization was measured to be about 55%. The statistical accuracy of the measurements is about $\delta P \sim 3\%$ for an 8-hour store in RHIC.

2. Event selection for the polarization measurements

The H-Jet Data Acquisition System (DAQ) records a 144 sample waveform with 2.4 ns sampling time for every triggered event [3]. The waveform analysis results in 2 measured parameters: amplitude A and time t. A typical distributions of measured time versus amplitude in a Si strip

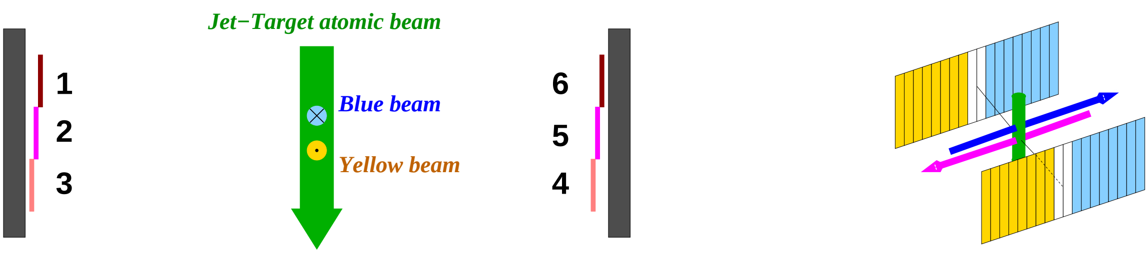

Figure 1: Schematic view of the atomic-beam of the jet-target, RHIC beam and six silicon detectors (left). Silicon detector division by strips (electronic channels), 8 strips per beam direction, is shown at the right picture.

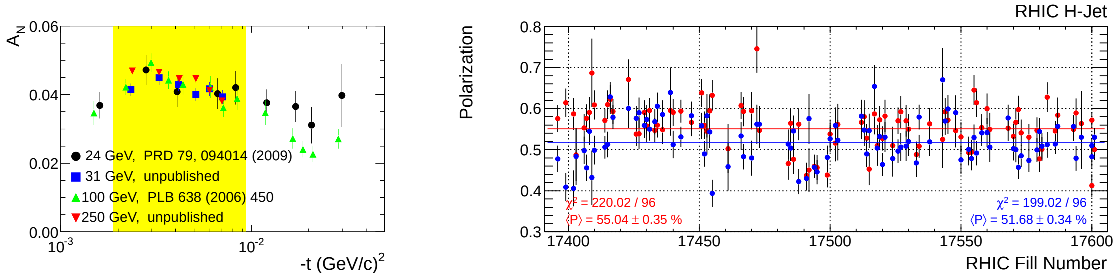

Figure 2: pp analyzing power measured with H-Jet (left) as a function of the beam energy and momentum transfer $-t = 2M_pT$. The recoil proton kinetic energy range $1 < T < 5$ MeV used for polarization measurements is highlighted. On-line results of Blue and Yellow beam polarization in RHIC Run13 (right).

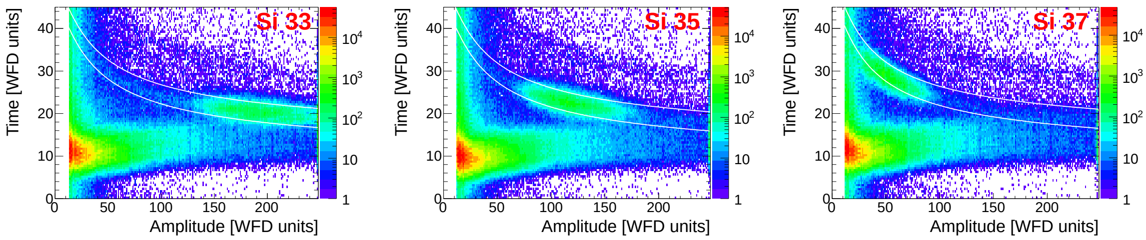

Figure 3: The dependence of measured time on signal amplitude. The low energy recoil proton regions are isolated by white lines. The recoil proton peak position depends on z-coordinate of the Si strip.

is shown on Fig. 3. The statistics is dominated by *prompts*, fast particles that punched through a Si detector. For the prompts, due to the Si stopping power dependence on the proton energy, the measured time t_{prompt} depends on the signal amplitude A as $t_{\text{prompt}} \approx t_0 + cA^p$ with $p \sim 2/3$. The peaks at $A \sim 10$ and $t \sim 10$ in the distributions in Fig. 3 are formed mostly by relativistic protons.

To isolate the low energy recoil protons which are stopped in the detector, one may compare the proton kinetic energy T with the time of flight:

$$\alpha A + E_{\text{loss}}(\alpha A, x_{DL}) = T = \frac{M_p L^2}{2(t - t_0)^2} \tag{2.1}$$

Here, M_p is proton mass, and $L \approx 78$ cm is the distance from the scattering point to the detector. To measure the time of flight $t - t_0$, the time offset t_0 has to be known. Energy $E_{\text{dep}} = \alpha A$ deposited in the active part of the detector is proportional to the gain α. A part of the proton energy E_{loss} , which is deposited in the detector entrance window (the *dead-layer*), does not contribute to the measured signal amplitude. Using the known stopping power dE/dx of silicon for protons [4], the energy losses E_{loss} in the dead-layer may be calculated as a function of detected energy αA and dead-layer thickness x_{DL}.

Thus, to identify recoil protons from the elastic pp scattering one has to know three calibration parameters t_0, α, and x_{DL} for every Si strip. These parameters are supposed to be determined in a calibration.

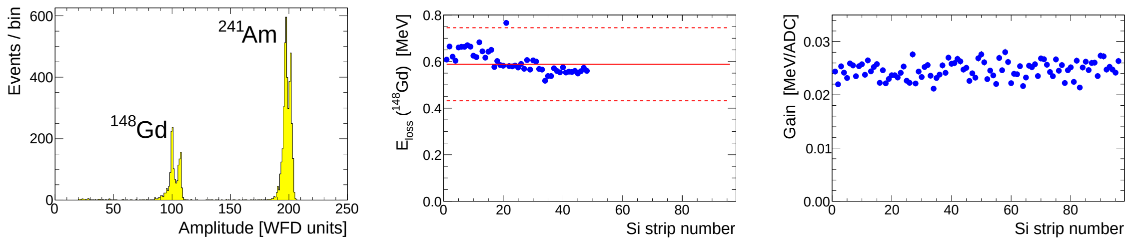

Figure 4: α-source signals in the H-Jet Si strip (left). Dead-layer thickness in units of energy lost by 148Gd alpha (center). The solid red line is the average dead-layer which is used for gain calculations in all strips. Distribution of gains in Si strips (right).

3. The H-Jet calibration

Since the analyzing power is internally measured in the H-Jet data analysis, the calibration is not essential for polarization measurements if recoil protons from elastic pp scattering can be well isolated. However, a precise calibration is important for suppression of the background related systematic errors in the polarization measurement. Traditionally, α-sources were used for the calibration [3]. Recently, two new methods were studied [6]. Neither of these methods allows us to determine all 3 calibration parameters. However, for every method, the missing parameters may be determined by minimizing the measured discrepancy in Eq. (2.1) for the elastic pp events.

3.1 Calibration using α-source

In special runs, the Si detectors are exposed by α-particles from ^{148}Gd (3.183 MeV) and ^{241}Am (5.486 MeV) sources. Two different energies of α-particles allow us to measure two calibration parameters α and x_{DL}. An example of such a calibration [5] is shown in Fig. 4.

Only left-side detectors (1–3) are exposed by Gd source. For these 48 channels, the average value of $\langle x_{DL} \rangle$ is calculated. For 48 right side channels only Am signal is available. The gain for these channels is calculated assuming that dead-layer in each strip is equal to $\langle x_{DL} \rangle$. Possible variations of the actual value of x_{DL} are included into the error of the determination of the gain.

3.2 Determination of t_0 by measuring the prompt time

Since most of events accepted by the DAQ are triggered by relativistic prompt particles (see Fig. 3), one may expect that mean measured time for all signal in a strip s differs from the t_0 by time of flight $\Delta t = L/c \approx 2.6$ ns where c is the speed of light

$$t_{\rm pr}^{(s)} = t_0^{(s)} + \Delta t \tag{3.1}$$

A more detailed analysis [7] shows that Δt is larger than the L/c by 1–2 ns because *(i)* actual velocity of prompt particles is smaller then speed of light c and *(ii)* due to charge collection effects in the Si detector the measured time for prompt particle is delayed by about 1 ns relative to the protons stopped in the detector.

The value of the measured mean time $t_{\rm pr}^{(s)}$ was found to be dependent on the amplitude cuts in the event selection. The dependence of average value $\langle t_{\rm pr} \rangle$ and RMS of the measured mean time $t_{\rm pr}^{(s)}$

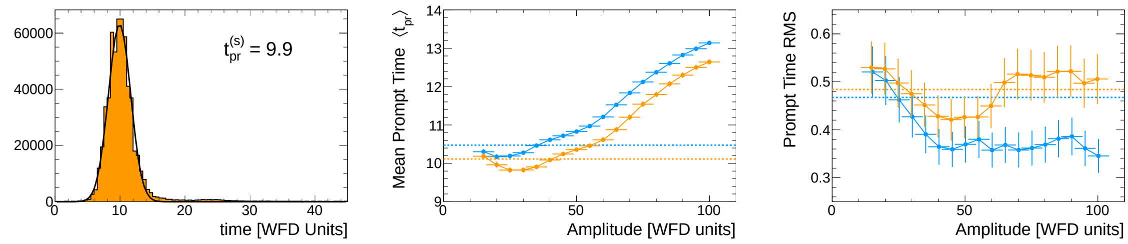

Figure 5: Distribution of the measured time for all events in one Si strip (left). Distribution of the mean values (center) and RMS (right) of measured time $t_{\rm pr}^{(s)}$ for all 96 Si strips are shown separately for the Blue and Yellow beams. Horizontal error bars show interval in amplitudes while vertical errors bars are widths of the corresponding distributions.

in all 96 strips on the signal amplitude cut is displayed in Fig 5. Since the RMS may be considered as quadratic sum of variations of signal delays in electronics and variations of systematic errors in measurements of $t_{\rm pr}^{(s)}$, only the signals with amplitude within 40–50 WFD units range were selected for calibration. The value of Δt, which is expected to be the same for all strips, may be determined by comparison of $t_{\rm pr}^{(s)}$ with the time offset $t_0^{(s)}$ found in *geometry based calibration*.

3.3 Geometry based calibration

Due to the geometrical orientation of the Si strips, every strip detects recoil protons produced at definitive angle only (see Figs. 1). This may be employed for a precise energy calibration of the detector. For elastic pp scattering, the z (along the beam) coordinate of recoil proton in the detector is related to the proton kinetic energy T as

$$z = L\sqrt{\frac{T}{2M_p}\frac{E_{\rm beam}+M_p}{E_{\rm beam}-M_p}} = \zeta\sqrt{T} \tag{3.2}$$

As a result, for a very narrow Si strip and linear dependence of the measured amplitude A on the proton kinetic energy, the distribution function

$$\eta(\sqrt{A}) = \left(\frac{d\sigma_{pp}}{dt}\right)^{-1}\frac{dN}{dA}, \tag{3.3}$$

is an image of the proton density profile in the jet which may be approximated by Gaussian distribution with $\sigma \sim 2.7$ mm . The amplitude $\sqrt{A_s}$ corresponding to the center of gravity of the function $\eta(\sqrt{A})$ is associated with the proton kinetic energy $T_s = (z_s/\zeta)^2$ calculated from the known z-coordinate of the Si strip. This conclusion remains valid with acceptable accuracy if we take into account the actual strip width (4.44 mm) and possible non-linearity of $A(T)$, e.g. due to energy losses in the dead-layer [6].

Obvious sources of the systematic errors in such a calibration are possible misalignment of detector position, beam angles, and holding field magnet. Due to the bending of a proton track in the magnetic field, the z-coordinate of the proton in the detector is shifted by $\Delta z = \pm b/\sqrt{2M_pT}$. The sign $\pm$ depends on left/right position of detector relative to the beam direction. For the H-Jet geometry, $b \approx 10\ \mathrm{cm}\cdot\mathrm{MeV}$. The alignment corrections should be accounted for in the data analysis.

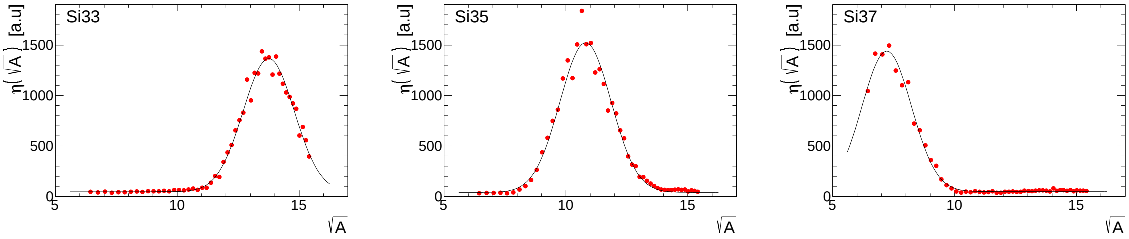

Figure 6: The measured function $\eta(\sqrt{A})$ for the same 3 strips as in Fig. 3 The distance between these strips centers is 8.9 mm.

These corrections may be routinely calculated by optimizing the consistency of the geometry based and the prompt time based calibrations.

After determination of the A_s and calculation of the elastic pp signal mean time t_s corresponding to the amplitude A_s, we can find the time offset $t_0^{(s)}$ by subtraction the time of flight:

$$t_0^{(s)} = t_s - L\sqrt{\frac{M_p}{2T_s}} \tag{3.4}$$

3.4 Comparison of the calibration methods

The value of Δt in Eq. (3.1) is supposed to be the same for all strips. It may be evaluated by comparing the results of geometry based and prompt based calibrations as shown in Fig. 7. This distribution allows one to make an estimate

$$\sigma_{t0}^{(g)} \oplus \sigma_{t0}^{(p)} = 0.36 \text{ ns}, \tag{3.5}$$

where $\sigma_{t0}^{(g)}$ and $\sigma_{t0}^{(p)}$ are accuracies of determination of t_0 in geometry and prompt calibrations, respectively, and $\oplus$ means quadratic summation.

The geometry based and α-source calibrations may be directly (i.e. without calculation of the time t_s) compared by considering the discrepancy $\delta_E = 2(T_s - E_\alpha(A_\alpha))/(T_s + E_\alpha(A_\alpha))$ (see Fig. 7):

$$\langle\delta_E\rangle = 0.0 \pm 0.3\%, \qquad \sqrt{\langle\delta_E^2\rangle} = \left\langle\frac{\sigma_T}{T}\right\rangle_{\text{geom}} \oplus \left\langle\frac{\sigma_T}{T}\right\rangle_\alpha = 1.6 \pm 0.3\% \tag{3.6}$$

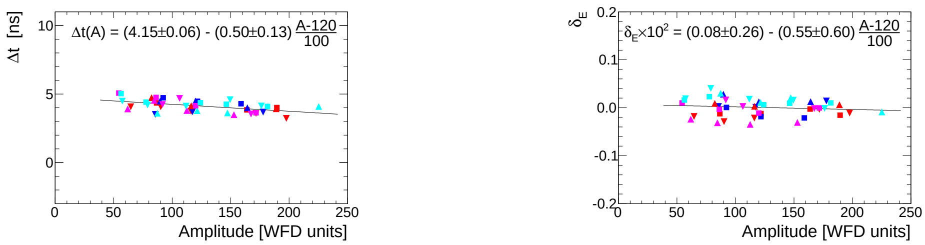

Figure 7: Comparison of geometry and prompt based calibration (left). Comparison of geometry based and α-source calibrations (right)

From these results, including also a comparison of the α-source and *prompt* calibrations, one can conclude that geometry based calibrations gives the best accuracy with a conservative estimate

$$\sigma_{t0}^{geom} \lesssim 0.2\ \text{ns}, \quad (\sigma_T/T)_{\text{geom}} \lesssim 0.7\% \sqrt{T/\text{MeV}} \tag{3.7}$$

Combining of all 3 methods of calibration may improve the accuracy of calibration by a factor 1.5–2.

At the moment, we have no good understanding of the Δt dependence on the signal amplitude. Eq. (3.6) forces us to conclude that the measured signal time depends on the amplitude. In other words, the time offset t_0 is amplitude dependent.

To summarize, 3 independent methods of the H-Jet calibration were developed. The geometry based calibration could be applied to only half of the silicon strips. However, together with prompt based calibration, these methods allows us to calibrate H-Jet in situ. In this case, the α-source calibration which requires a stand alone measurement could be used only for a pre-calibration of the H-Jet and for verification of the results of other 2 methods.

4. Systematic errors in the H-Jet polarization measurement

Flipping polarities of the proton beams and hydrogen target jet in the measurements allows us to strongly suppress systematic errors due to the beam intensity and acceptance asymmetries. Two remaining sources of systematic errors are uncertainty in the hydrogen jet polarization and beam gas scattering background.

4.1 Uncertainty in the hydrogen jet polarization

The Breit-Rabi polarimeter monitors the atomic hydrogen polarization $P_{\text{jet}}^{(atom)} \approx 0.958$ in the jet with a high accuracy. A measured [2] $(3.5 \pm 2.0)\%$ contamination of the jet by hydrogen atoms bound into unpolarized proton molecules results in a dilution of the average jet protons polarization to the value of $P_{\text{jet}} = 92.4 \pm 1.8\%$. Relatively large error in measurement of the molecular hydrogen admixture and the absence of permanent monitoring of this parameter results in the biggest systematic uncertainty in the polarization measurement with the RHIC H-Jet.

4.2 Background related systematic errors

About $r \approx 5\%$ of events selected for polarization measurements come from beam proton interactions with the beam gas. Such events are not correlated with jet polarization, but may contribute to the a_{beam} measurement with effective analyzing power $A_N^{(\text{bgr})}$. As a result, the beam polarization will be measured with an error

$$P_{\text{meas}} = P_{\text{beam}} \left(1 + rA_N^{\text{bgr}}/A_N\right) \tag{4.1}$$

It was found in earlier studies that $A_N^{\text{bgr}} \approx 0$ and, thus, background does not affect the polarization measurement. To check this results, two methods are being employed.

The time of signal detection is divided on 110 ns intervals associated with the RHIC beam bunches. For some bunches only one beam, Blue or Yellow, is scattered on the jet protons. In this

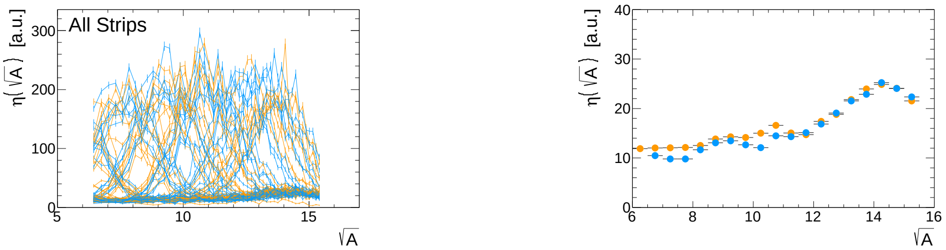

Figure 8: Superimposed $\eta(\sqrt{A})$ distributions for all H-Jet Si strips (left). A common part of the distributions which may be associated with background is shown separately for Blue and Yellow beams (right). The example is given for the RHIC fill 17247 with increased background due to the issue with vacuum pump.

case only background events will be detected in the strips corresponding to the absent beam. In addition, special measurements with one beam only were performed in the RHIC Run13.

The second method is based on detailed study of the $\eta(\sqrt{A})$ distribution in all strips. One can expect that in every Si strip this distribution includes the jet density profile which position depends on the strip z-coordinate and a background which is expected to be the same for all strips. If so, the background contribution may be experimentally isolated (see Fig. 8) and properly subtracted.

5. Summary

The RHIC H-Jet polarimeter provides reliable measurements of the average beam polarizations. Several calibration methods were developed which allow us to monitor energy calibration with a percent accuracy as well as to make a precise alignment of the detectors. Study of background due to the beam gas is underway. Molecular hydrogen in the Jet gives the largest uncertainty in the polarization measurements.

Acknowledgments

This work is performed under Brookhaven Science Associates, LLC, contract No. DE-AC02-98CH10886 with the U.S. Department of Energy. Funding is also provided from the RIKEN BNL Research Center.

References

[1] I. Alekseev *et al.* NIM **A499** (2003) 392;

[2] H. Okada *et. al.*, Phys.Lett. **B638** (2006) 450.
I. G. Alekseev *et. al.*, Phys. Rev. **D79**:094014,2009

[3] Hiromi Okada, *Measurement of the Analyzing Power A_N in pp Elastic Scattering in the CNI Region with a Polarized Atomic Hydrogen Gas Jet Target*, PhD Thesis. Kyoto University 2006 http://www.bnl.gov/userscenter/Thesis/2007/Okada_Thesis.pdf

[4] http://physics.nist.gov/PhysRefData/Star/Text/PSTAR.html

[5] K. O. Eyser, private communication.

[6] A.A. Poblaguev, *A precise in situ calibration of the RHIC H-Jet polarimeter* (unpublished).

[7] A.A. Poblaguev, *Waveform dependence on signal amplitude in the RHIC H-Jet polarimeter*, (unpublished).